

# Selective chemical surface modification of fluidic microsystems and characterization studies

Stefanie Breisch<sup>1</sup>, Bas de Heij<sup>3</sup>, Markus Löhr<sup>2</sup>  
and Martin Stelzle<sup>1,4</sup>

<sup>1</sup> Naturwissenschaftliches und Medizinisches Institut, Markwiesenstrasse 55,  
D-72770 Reutlingen, Germany

<sup>2</sup> Hahn-Schickard Institut für Mikro- und Informationstechnik, Wilhelm-Schickard-Straße 10,  
D-78052 Villingen-Schwenningen, Germany

<sup>3</sup> University of Freiburg, Institut für Mikrotechnik IMTEK, Georges-Köhler-Allee 101-103,  
D-79110 Freiburg im Breisgau, Germany

Received 12 September 2003

Published 9 January 2004

Online at [stacks.iop.org/JMM/14/497](http://stacks.iop.org/JMM/14/497) (DOI: 10.1088/0960-1317/14/4/009)

## Abstract

Control of wetting behaviour of fluidic microsystems was achieved by selective chemical surface modification using either a solution-based procedure or micro-contact printing. The modification procedures were designed in such a way as to obtain optimum wetting in fluid channels, sample reservoirs and nozzles, while at the same time preventing intermixing of fluids from different nozzle exits and thus enabling multiple long-term stable delivery of nano-litre droplets. Analysis included thickness measurements by ellipsometry, contact angle measurements and fluorescence microscopy. Selectively coated TopSpot dosage chips as are used for the fabrication of DNA and protein micro-arrays exhibit superior performance over uncoated dosage chips. Mixed and back-filled silane coatings show enhanced stability versus hydrolysis in basic and acidic solutions, as has been determined from measurements of contact angle as a function of immersion time.

## 1. Introduction

TopSpot dosage chips are used for the fabrication of DNA- and protein micro-arrays [1] (figure 1). There, systems for massive parallel liquid handling and delivery in nano- to pico-litre quantities are required.

As dimensions shrink, wetting properties of fluidic systems become increasingly important, since the ratio between interaction area of a particular fluid volume with interfaces and the fluid volume itself increases. In the past, a large variety of fluidic microsystems have been fabricated from silicon and glass because of the advantageous wetting properties of these materials as far as aqueous solutions are concerned. In particular, electrophoresis on a chip has been thoroughly investigated [2–9]. However, while fluid channels, sample wells and nozzles require reliably wettable surfaces,

intermixing of different fluids and deterioration of droplet formation properties due to uncontrolled wetting may result in serious limitations to the performance of these devices. In case of the TopSpot dispenser we could show that a hydrophobic, i.e. non-wettable coating, selectively applied to the bottom nozzle plate of the chip, can provide an effective remedy.

There have been numerous reports about the use of silane derivatives to chemically modify surfaces of glass or silicon oxide. Important applications thereof concern specific modifications of the stationary phase in gel chromatography [10–15], biochips [16–18] and micro-fluidic devices such as electrophoresis chips [13, 19]. In many studies, the importance of well-controlled preparation conditions, namely with respect to ambient humidity and surface hydration is emphasized [20–25]. Low humidity atmosphere is especially critical if highly reactive chloro-silane derivatives are to be employed. In order to obtain reproducible results, this usually requires inert gas conditions of a glove box equipped with silica absorber as was used in our study throughout.

<sup>4</sup> To whom correspondence should be addressed.

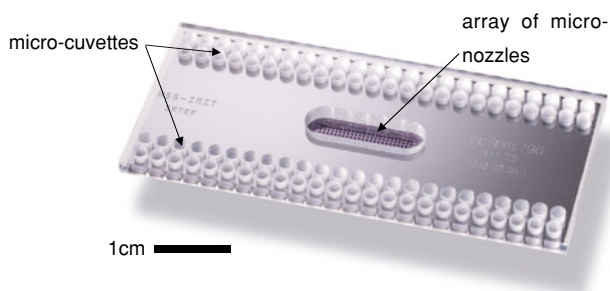
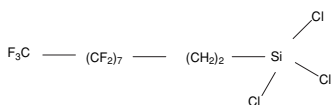


**Figure 1.** TopSpot print-head consisting of a glass/silicon hybrid structure with micro-cuvettes on the top side, embedded micro-channels and an array of micro-nozzles at the centre of the chip.

1H,1H,2H,2H-perfluorodecyltrichlorosilane (PFTCS),  $M = 581,56 \text{ g/mol}$



trifluoropropyltrichlorosilane (TPT),  $M = 231,50 \text{ g/mol}$

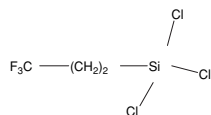


**Figure 2.** Silane derivatives used for coating of micro-fluidic devices.

In the following we will present materials and methods used for coating as well as for analysis of coatings. Further, in the results and discussion section, chemical stability of coatings fabricated by various procedures is investigated, with a particular focus on mixed and back-filled silane coatings. In addition, a stamp based coating procedure and preliminary results are presented. Finally, the spotting performance of a micro-dispenser chip is demonstrated.

## 2. Materials and methods

### 2.1. Modification agents and solutions

Silane derivatives (figure 2) were obtained from ABCR (Karlsruhe, Germany) and used as received. Hexane and toluene were obtained from Fluka (Taufkirchen, Germany) or Roth (Karlsruhe) with a water content of  $<0.005\%$  (vol:vol). A tri-functional fluoro-carbon terminated silane (1H,1H,2H,2H-perfluorodecyltrichlorosilane, PFTCS) was used in solutions of hexane to create surfaces with teflon-like properties. PFTCS has previously been investigated with respect to packing density as a function of process parameters [26] in a study concerned with gas phase deposition of silanes. Solutions of trifluoropropyltrichlorosilane (TPT), in hexane were employed to study the efficiency of backfilling with small molecules towards increased hydrolytic stability of PFTCS [14, 27]. Also the merits of co-deposition of a long-chain molecule such as PFTCS and a small silane derivative, TPT, were investigated. Unless stated otherwise, silane concentration was  $0.02\%$  (vol:vol) in all cases.

### 2.2. Coating procedure in solution and set-up

Prior to the coating process silicon oxide and glass surfaces were cleaned in a solution of  $\text{H}_2\text{O}_2/\text{NH}_4$  (33%)/ $\text{H}_2\text{O}$  (1:1:5 vol:vol:vol) at  $80^\circ\text{C}$  for about 30 min, extensively rinsed in MilliQ water and isopropanol and finally dried under an IR light source. Alternatively, chips were treated in an  $\text{Ar}/\text{O}_2$ -plasma at about  $5 \text{ W cm}^{-2}$  for 3 min and immersed in MilliQ water for at least 30 min. Both of these pre-conditioning methods render surfaces with sufficient density of silanol groups for silane derivatives to form covalent siloxane bonds that results in a dense layer.

In order to ensure reproducible results of coating by highly reactive chloro-silane derivatives great care must be taken to ensure the absence of water both in solvents used and in the process environment. Therefore, all reactions were performed in a glove box under dry nitrogen atmosphere at room temperature. The glove box comprised a gas-cleaning system including a silica/copper absorber to remove both moisture and oxygen. The absorber was regenerated regularly (typically every one to three months) and a vacuum interlock was used to introduce materials and chips into the system and prevent moisture from contaminating the atmosphere.

TopSpot chips are mounted in a custom designed chip carrier with Viton gaskets to provide a gas and solution tight seal between the front (cuvette) side and the bottom (i.e. nozzle) side of the chip.

Inert gas is supplied to the cuvette side of the chip and flows through the micro-channels and nozzles, thus preventing coating solution from entering into the micro-fluidic device. In this way, only the bottom side is modified by the coating solution, while channels and nozzles remain hydrophilic. After retrieving the chip carrier from the coating solution and rinsing in pure solvent, gas flow is maintained for about 10 min until the chips and the chip carrier are completely dry. This is to prevent residual solution from creeping into nozzles or channels.

Finally, the coating process is concluded by the heating of the coated devices under an IR (infra-red) lamp to about  $120^\circ\text{C}$  for about 30 min to allow for complete formation of Si–O–Si bonds.

Contact angle of the bottom surface of coated micro-systems and spontaneous filling of channels and nozzles are tested to verify for proper coating.

Optimization of process conditions was achieved using silicon wafers with a 500 nm TEOS (tetraethylorthosilicate) oxide layer as a substrate. The process parameters obtained thereof were then applied to the selective coating of micro-fluidic devices.

### 2.3. Micro-contact printing ( $\mu\text{CP}$ )

In an attempt to reduce the complexity and cost of device fabrication, fluidic micro-systems have been fabricated comprising open channels to guide fluid from micro-cuvettes on the front side of a chip to micro-nozzles on the bottom side [1]. These systems allow for parallel dispensing of nano-litre droplets. However, in order to prevent solution from creeping from the channels and possibly intermixing with solutions contained in adjacent channels, the bottom side of the chip has to be modified with a non-wettable coating. Obviously,

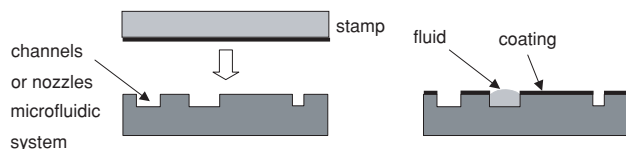


**Figure 3.** Coating of fluidic microsystems comprising open channels by micro-contact printing.

the previously described process using pressurized inert gas cannot be applied in this case. Instead, direct application of the modifying agent by micro-contact printing ( $\mu$ CP) is used (figure 3). Again a solution of a silane derivative is employed. However, instead of immersing the chip, a stamp fabricated from a suitable polymer is wetted with the solution. After the solvent has evaporated completely, the stamp is pressed onto the chip, thus bringing the elevated structures of the chip in contact with the modifying agent. Typical pressures are of the order of 1–10 N. However, on flat surfaces such as polished silicon wafers, even lower pressure may suffice to bring both surfaces into intimate contact, a condition which is indicated by dark appearance of the interface and the absence of interference fringes. Within seconds, a hydrophobic coating is formed, while the channels remain hydrophilic. Again an IR lamp or oven is used to bring the formation of Si–O–Si bonds to completion.

The choice of the stamp material depends on the solvent to be used. Hexane and a silicone elastomer (Sylgard 184, Dow Corning) has been identified as good combination, since this elastomer tends to swell and take up the silane solution in a sponge type fashion. In addition, this material is elastic and may adapt to minor topological variations of the surface.

## 2.4. Analysis of coatings

**2.4.1. Ellipsometry.** For a complete account of this method and its applications particularly to the analysis of monolayer coatings the reader is referred to a large body of original literature [28, 29]. Briefly, ellipsometry uses the reflection of monochromatic polarized light to probe optical properties, i.e. refractive index, absorbance and thickness of thin layers on reflective substrates. The sensitivity is high enough to even monitor the self-assembly of monolayer coatings. In the context of this study, ellipsometry was used to determine the time course of silane deposition from solution by measuring the change in reflection properties prior and after immersion in the reaction solution for a variety of durations.

**2.4.2. Contact angle measurement.** Contact angles were determined by bringing droplets of deionized water into contact with the surface of the sample while monitoring the angle between the surface of the sample and the tangent drawn to the contour of the droplet through an ocular (figure 4). Both advancing and receding contact angles were determined using the goniometer built into the ocular. A detailed description of this method and its theoretical background may be found in Adamson and references cited therein [30]. Basically, according to Young's equation the contact angle,  $\theta$ , is a

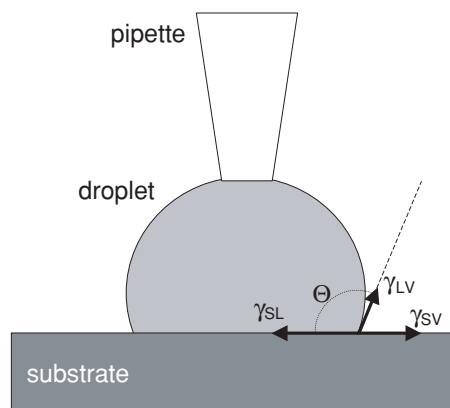


**Figure 4.** Illustration of contact angle formed by a droplet of water on the surface of the substrate. Hydrophobic, i.e. non-wettable surfaces exhibit large, hydrophilic, i.e. wettable surfaces in contrast show small contact angles.

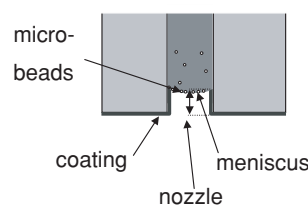


**Figure 5.** The position of the meniscus of fluid in micro-nozzles was determined using fluorescent micro-beads immersed in a solution of water/sucrose. Since the specific weight of particles exceeds that of the solutions, particles rinsed to the nozzle tend to accumulate at the air/solution interface, thus marking the position of the meniscus. With the  $2\ \mu\text{m}$  particles used in this study, a precision of position measurement of  $<\pm 3\ \mu\text{m}$  was achieved.

function of the interfacial tensions between the solvent, sample and vapour:

$$\cos \theta = \frac{(\gamma_{SV} - \gamma_{SL})}{\gamma_{LV}} \quad (1)$$

with  $\gamma_{SL}$ ,  $\gamma_{SV}$ ,  $\gamma_{LV}$  denoting the interfacial tension between solid and liquid phase, solid and vapour phase, and liquid and vapour phase, respectively.

Hydrophobic, i.e. non-wettable surfaces exhibit large contact angles whereas hydrophilic, i.e. wettable surfaces show small contact angles when probed with water. The hysteresis between advancing and receding contact angle reveals heterogeneity of the surface. This may be due to either lateral variations of the chemical composition of the coating or surface roughness [31–33]. Thus, contact angle measurement provides a tool to assess the coverage and integrity of ultra-thin coatings.

**2.4.3. Fluorescence microscopic detection of meniscus level.** Fluorescence microscopy was used as a further means to characterize ultra-thin coatings on micro-fluidic devices, particularly to detect the position of the meniscus within nozzles and thus relate process parameters to the distance up to which the reagent solution may enter into the nozzles during the deposition process. The measurement procedure is shown in figure 5. Fluorescently labelled latex beads ( $2\ \mu\text{m}$  diameter)

**Table 1.** Coating process parameters and contact angles obtained after 30 min and 24 h immersion in silane solution, respectively.

| Exp. no.       | Silane    | T (°C) | C (%)     | $\theta_{adv}$ (30 min) (°) | $\theta_{rec}$ (30 min) (°) | $\theta_{adv}$ (24 h) (°) | $\theta_{rec}$ (24 h) (°) |
|----------------|-----------|--------|-----------|-----------------------------|-----------------------------|---------------------------|---------------------------|
| 1              | PFTCS     | 22     | 0.5       | 105                         | 61                          | —                         | —                         |
| 2              | PFTCS     | 23     | 0.5       | 112                         | 66                          | —                         | —                         |
| 3              | PFTCS     | 21     | 0.08      | 120                         | 90                          | —                         | —                         |
| 4              | PFTCS     | 22     | 0.02      | 121                         | 90                          | —                         | —                         |
| 5              | PFTCS     | 0      | 0.017     | 115                         | 92                          | —                         | —                         |
| 6              | PFTCS     | 22     | 0.02      | —                           | —                           | 125                       | 108                       |
| 7              | TPT       | 22     | 0.02      | —                           | —                           | 86                        | 58                        |
| 8 <sup>a</sup> | TPT/PFTCS | 22     | 0.02/0.02 | —                           | —                           | 116                       | 90                        |
| 9 <sup>a</sup> | PFTCS/TPT | 22     | 0.02/0.02 | —                           | —                           | 119                       | 90                        |

<sup>a</sup> Backfilled layers: substrates coated with first silane for 24 h and subsequently immersed in solution of second silane for 24 h.

were mixed in a small concentration with a mixture of water and sucrose. The addition of sucrose is necessary to adjust the density of solution and beads and allow for slow sedimentation of beads to occur. The micro-cuvettes of the TopSpot chip were filled with this mixture, causing some of the beads to be rinsed towards the nozzles. Since the specific weight of the particles exceeds that of the solvent, particles reaching the nozzle accumulate precisely at the meniscus of the fluid. Using the z-dial of the microscope drive, the distance between the bottom surface of the fluidic chip and the meniscus may be determined by first focussing on the nozzle rim and afterwards on the particles. The 2  $\mu\text{m}$  particles used in this study enabled a precision of position measurement of  $<\pm 3 \mu\text{m}$ .

### 3. Results and discussion

#### 3.1. Solution based procedure

Silicon slides (2 cm  $\times$  1 cm) with 500 nm oxide layer were used in coating experiments to determine optimum process parameters, namely (1) duration of treatment, (2) concentration of silylating agent and—in the case of coating of printing heads only—(3) the inert gas pressure during immersion in the reaction solution. Layer thickness was determined by ellipsometry and surface properties were assessed by contact angle measurement.

#### 3.2. Duration of treatment and concentration of silylating agent

A typical measurement of contact angle and thickness determined by ellipsometry as a function of time is shown in figure 6. In each experiment a number of slides was immersed into the well-stirred reaction solution under inert gas conditions and retrieved consecutively after a reaction time varying from 10 s to 180 min, rinsed in pure solvent and dried. The concentration of the silane in the reaction solution varied from 0.02% to 0.5% (vol) and was 0.08% in case of figure 6. With all samples, even for the smallest reaction time, a high contact angle of  $>100^\circ$  is observed, indicating rapid and almost complete coverage of silane molecules. According to ellipsometry, the thickness reaches a plateau after only a few minutes. There are, however, also indications of additional deposition upon prolonged exposure

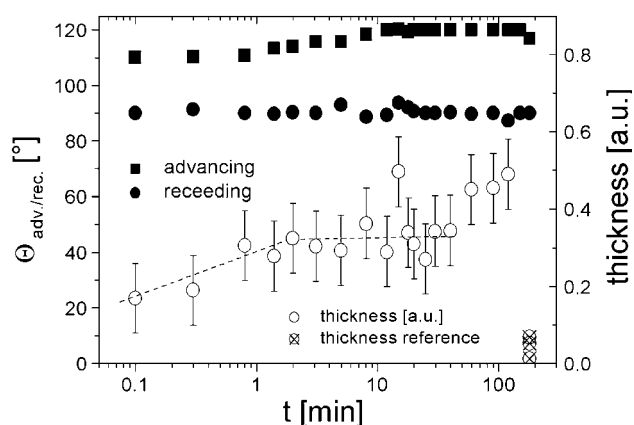


**Figure 6.** Typical result of a coating experiment, using PFTCS (0.08% in hexane) on oxidized silicon showing contact angle and layer thickness as a function of treatment time. A set of substrates was pre-treated and immersed in the solution at  $t = 0$ . Samples were consecutively retrieved from the coating solution and subsequently contact angle and thickness of the layer were measured. Dotted lines are intended as guides for the eye and indicate a plateau in the thickness after only a few minutes of treatment.

( $>1$  h) to the coating solution, presumably through the built-up of siloxane multilayers. Advancing contact angles of up to  $122^\circ$  were measured while receding angles were about  $60$ – $90^\circ$ . Interestingly, the hysteresis between advancing and receding angles decreased with decreasing concentration of silane. Generally, such hysteresis is indicative either for roughness [31, 32] or for chemical inhomogeneity of the surface [33]. Since polished silicon wafers were used as samples, a chemical inhomogeneity of the coating due to three-dimensional polymerization of silane when supplied in high concentration is considered the most probable explanation of the observed hysteresis. According to Brzoska *et al* low hysteresis is also related to high stability against chemical attack [33]. While after 30–60 min peak values of the advancing contact angle are reached, receding contact angle increases further. In summary, samples exposed to relatively low concentration of silane for prolonged duration (24 h) yield the most homogeneous coatings as is indicated by low hysteresis and high chemical stability. Results are summarized in table 1.

### 3.3. Chemical stability of coatings, backfilling with small molecules and horizontal polymerization using mixtures of small and long-chain silane derivatives

Silane derivatives bind to oxide surfaces via siloxane bonds (Si–O–Si), which may be hydrolyzed in aqueous solution at acidic or basic pH values. Accordingly, shielding these bonds from hydrolytic attack by introducing hydrophobic moieties is expected to enhance the chemical stability of the monolayer coating [34]. Wirth *et al* reported enhanced stability in monolayers backfilled with small molecules or deposited from a mixture of molecules of different sizes and discussed their use as chromatography stationary phases [14, 27]. In particular, they used poly-functional silane derivatives in order to utilize their cross-linking capability.

Our goal in this study was to develop a coating for micro-fluidic components with enhanced stability in both acidic and basic aqueous solutions. Considering the relatively high cost of micro-fluidic systems fabricated from silicon or glass, multiple uses of such devices with repeated intermediate cleaning cycles are desirable. Ideally, the user of such a system should not have to apply a fresh coating frequently but rather be able to use the initial coating over the entire life span of the micro-system. However, some of the more efficient cleaning procedures involve basic or acidic aqueous solutions. We therefore focussed on this aspect of chemical stability in this study.

Four different types of experiments were performed. Firstly, the coatings of the pure compounds, PFTCS and TPT, were applied and their stability upon immersion in hydrochloric acid ( $c = 32\%$ ) and sodium hydroxide solution ( $c = 1\text{ M}$ ) was investigated (figures 7(a)–(d)). Secondly, mixed monolayers were prepared by subsequent deposition of the long chain derivative, PFTCS, and the small derivative, TPT (figures 7(e), (f)). In a third set of experiments, at first TPT and subsequently PFTCS was deposited (figures 7(g), (h)). Finally, samples were immersed in mixtures of PFTCS and TPT (90% : 10%) to obtain co-adsorbed monolayers (figures 7(i), (j)). The layer quality and stability was assessed by contact angle measurements. Each point corresponds to a sample that has been immersed in either acidic or basic solution for the given duration. Deterioration of the coating was quantified by fitting an exponential decay curve with offset to the data. Decay times as well as offset values are summarized in table 2.

All types of coating investigated here show some degree of deterioration when brought in contact with basic or acidic solutions. Generally, the effect of the basic solution is more pronounced than that of HCl. Even with the pure PFTCS monolayer, the advancing contact angle remains above  $105^\circ$  after 60 min in 32% HCl (figure 7(b)), while considerable deterioration is observed in NaOH (figure 7(a)). When comparing these results with TPT (figures 7(c), (d)), it is apparent that chain length plays a significant role in shielding the siloxane bonds from chemical attack. The TPT layer shows much lower contact angle initially and decay times are considerably smaller in both NaOH and HCl. Interestingly, however, the surfaces do not become completely wettable but attain a certain final offset value of the contact angle.

Coatings obtained by either backfilling or co-deposition show enhanced stability when compared to coatings consisting

**Table 2.** Contact angles obtained with pure and mixed silane coatings after deposition and stability of these coatings versus chemical attack by 1 M NaOH and 32% HCl, respectively.

| Silane              | Medium | $\tau_{adv}$ | Offset      | $\tau_{rec}$ | Offset      |
|---------------------|--------|--------------|-------------|--------------|-------------|
| PFTCS               | NaOH   | 16.6         | $70 \pm 5$  | 13.2         | $43 \pm 4$  |
|                     | HCl    | 7.2          | $105 \pm 2$ | 3.8          | $86 \pm 2$  |
| TPT                 | NaOH   | 2.4          | $27 \pm 2$  | 2            | $16 \pm 3$  |
|                     | HCl    | 1.2          | $46 \pm 2$  | 1.3          | $28 \pm 2$  |
| PFTCS <sub>bf</sub> | NaOH   | 10.2         | $92 \pm 2$  | 18.6         | $52 \pm 3$  |
|                     | HCl    | 11.6         | $104 \pm 3$ | 18           | $64 \pm 5$  |
| TPT <sub>bf</sub>   | NaOH   | 15.8         | $85 \pm 3$  | 44           | $33 \pm 13$ |
|                     | HCl    | 2.0          | $105 \pm 2$ | 7.5          | $74 \pm 2$  |
| HP:TPT/PFTCS        | NaOH   | 25           | $94 \pm 5$  | 20           | $60 \pm 4$  |
|                     | HCl    | 22           | $101 \pm 5$ | 15           | $60 \pm 3$  |

PFTCS<sub>bf</sub>: backfilling of a TPT coated surface by immersing in a PFTCS solution.

of only one type of silane. The backfilled layers show the same initial contact angles regardless of the deposition order, indicating that predominantly PFTCS is the main constituent at the interface to the solution. However, long-term stability and final contact angle of TPT/PFTCS<sub>bf</sub> (figures 7(g), (h)) is slightly but significantly higher than in the case of the opposite deposition order (figures 7(e), (f)).

Quite similar results were obtained by co-deposition of TPT and PFTCS (figures 7(i), (j)). Due to its lower molecular weight and related higher mobility, it is to be expected that TPT to a large degree will form the initial coating of the surface while PFTCS molecules may fill in gaps and provide for a high contact angle and enhanced shielding of siloxane bonds. The behaviour of a monolayer obtained from co-deposition of TPT and PFTCS should thus be comparable to that of a TPT layer back-filled with PFTCS, which in fact it is.

In summary, a considerable improvement in the stability of silane coatings with respect to basic solutions was achieved by employing backfilling or co-deposition from mixtures of different silane derivatives. The deposition processes are applicable to the coating of micro-fluidic devices such as the TopSpot system.

### 3.4. Analysis of nozzle coating versus inert gas pressure

The degree of undesired coating of inner surfaces adjacent to the nozzle outlet was assessed using fluorescent micro-beads and an inverted fluorescence microscope. Thus, the distance between the rim of the nozzle (visible due to residual fluorescent contaminants) and the relative position of the fluid meniscus within the nozzle could be determined. An example is displayed in figure 8. In the micrograph in figure 8(a) the focus was adjusted to the rim of the nozzle while figure 8(b) shows the focus adjusted such as to image the fluorescent micro-beads which accumulate at the fluid/air interface (figure 4).

Clearly and as expected, the gas flow applied during the deposition process has a pronounced influence on the position of the meniscus as can be seen in figure 8(c). The higher the pressure and accordingly the velocity of the inert gas stream the smaller the penetration depth of the reaction solution into the nozzle. In the case of the TopSpot chips considered

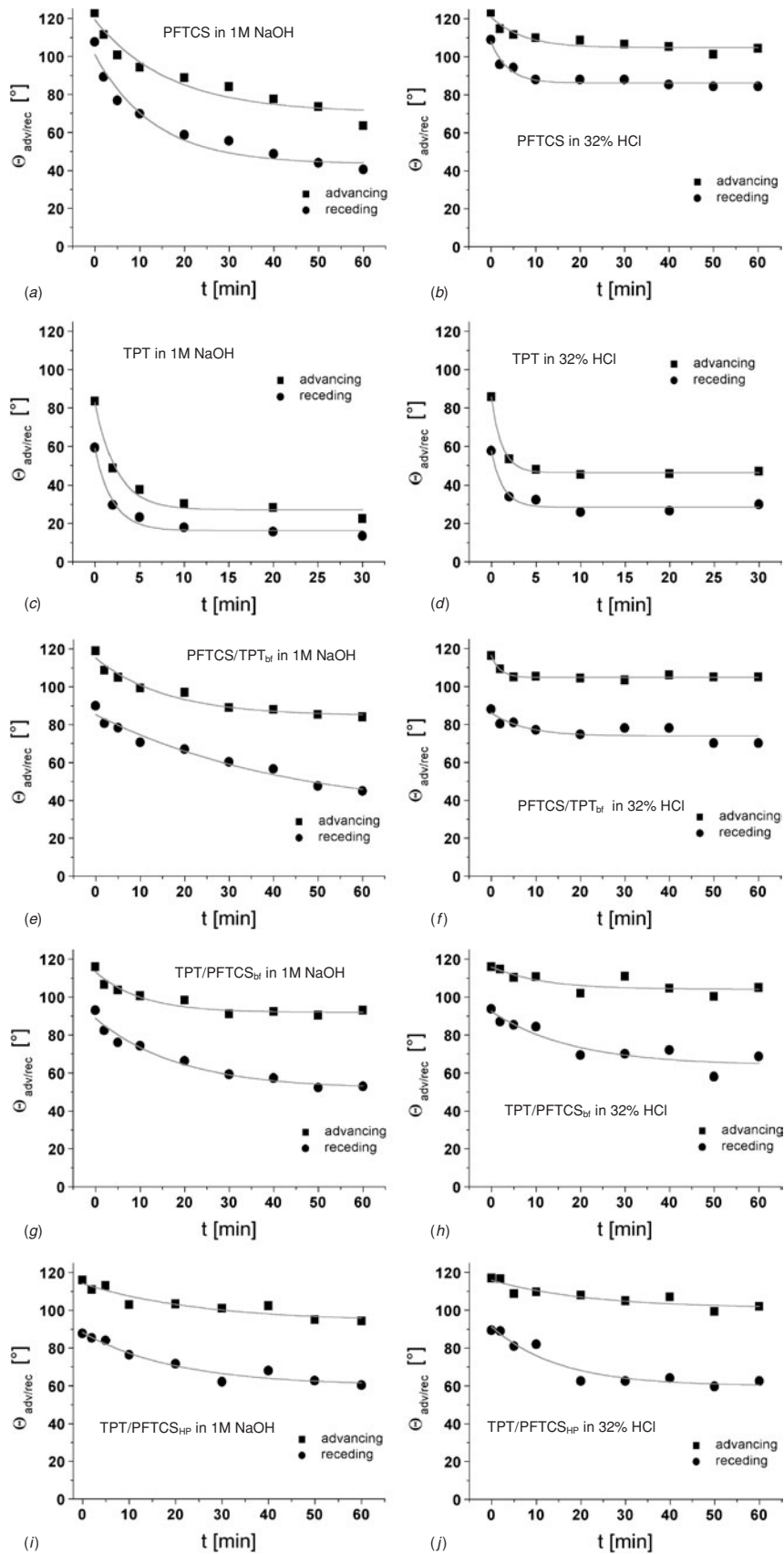


**Figure 7.** Stability of coatings versus acidic (32% HCl) and basic (1 M NaOH) solutions as a function of time for various compositions and fabrication processes. (a), (b) pure PFTCS, (c), (d) pure TPT, (e), (f) PFTCS backfilled with TPT, (g), (h) TPT backfilled with PFTCS, (i), (j) co-deposition from a mixture of PFTCS (90%) and TPT (10%) at a total silane concentration of 0.02%.

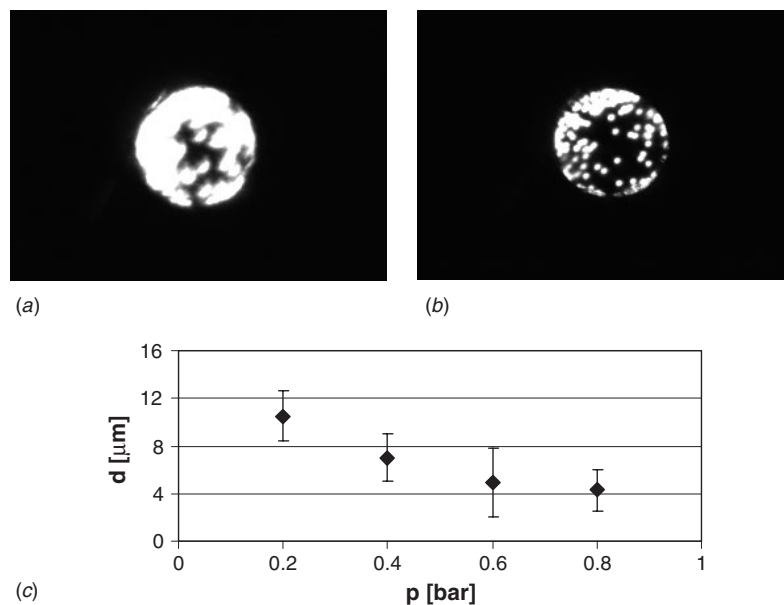


**Figure 8.** Micrographs of nozzles filled with aqueous solution containing fluorescent micro-beads: (a) focus on rim of nozzle, (b) focus on beads accumulated at air/solution interface. (c) Distance between nozzle rim and meniscus of fluid as a function of inert gas pressure during the coating process. As pressure increases, the depth to which solvent may enter into the nozzle causing undesired deposition of a hydrophobic silane layer decreases.

here (nozzle diameter:  $50 \mu\text{m}$ ) saturation is approached for a pressure level above approx. 0.5 bar with a minimum penetration depth of  $4 \mu\text{m}$ .

### 3.5. Micro-contact printing

**3.5.1. Printing procedure results.** Micro contact printing was performed using the same reaction solution of PFTCS in hexane. It proved, however, very important to have the stamp dry very thoroughly after adding reaction solution prior to printing. Otherwise, residual solvent will creep into the open channels and cause undesired deposition of coating agent and render the channels more or less hydrophobic as well. During the printing process, pressure applied must be high enough to ensure perfect contact between stamp and surface over the entire surface area. Since the elastomer is transparent, this may easily be monitored visually. During approach of the elastomer surface towards a planar and smooth surface, firstly interference colours appear followed by homogeneous dark appearance of the interface when both surfaces come into contact.

The surfaces were kept in contact for at least 30 s in order to allow some degree of diffusion of silane molecules in order to form a monolayer as complete as possible.

**3.5.2. Channel filling.** Apart from the contact angle measurement on the bottom surface the spontaneous filling of the channels is the critical criterion for proper function of the TopSpot device. In figure 9, a micrograph of the bottom side of a TopSpot chip with open channels is shown. Four of six channels whose respective micro-cuvettes located on the opposite side of the chip had previously been filled with a coloured aqueous solution show spontaneous delivery of fluid along the open channels and into the nozzles. At the same time, no overflow or cross-contamination towards adjacent channels

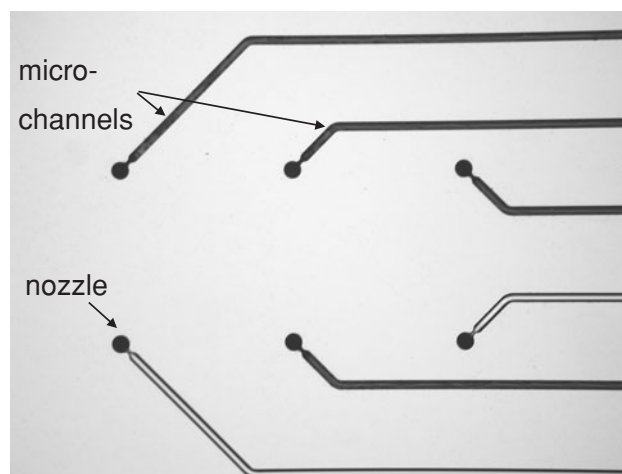


**Figure 9.** Micrograph of bottom face of TopSpot chip showing open micro-channels connecting to nozzles. Micro-cuvettes located on the opposite side of the chip had previously been filled with a dye stained aqueous solution. Spontaneous filling and proper containment of fluid within the channels is observed in four channels appearing dark in the micro-graph. In contrast, two of the channels appearing bright do not contain any fluid.

is observed, indicating proper function of the hydrophobic coating.

In summary, these results show the feasibility of controlling the wettability of micro-fluidic devices with open channels by micro-contact printing.

### 3.6. Spotting performance of selectively coated TopSpot chips

Selectively coated TopSpot print-heads exhibit superior homogeneity and reliability with respect to formation and dispensing of nano-droplets.

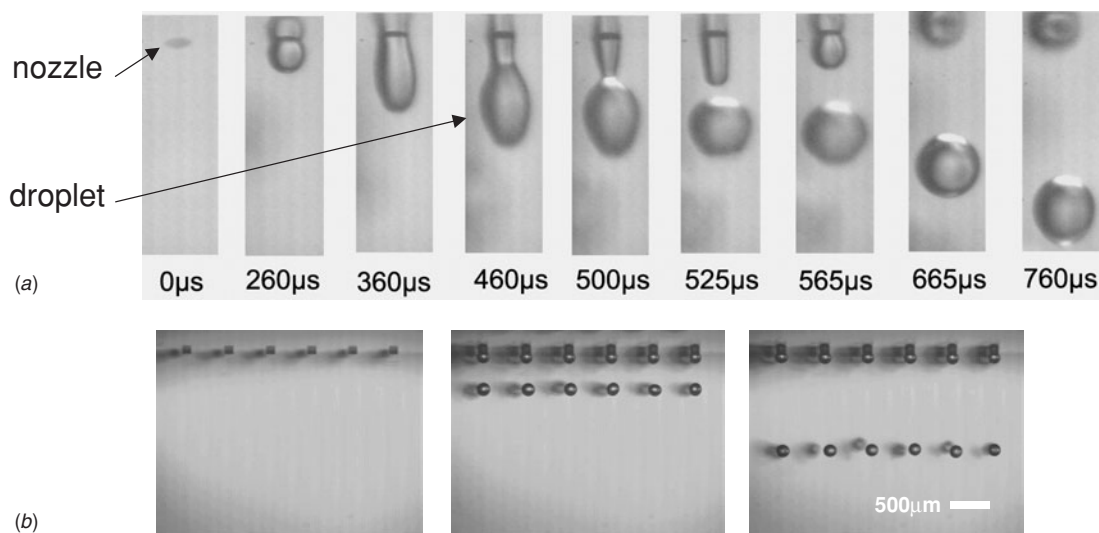


**Figure 10.** (a) Micrographs of droplet dispensing from a coated TopSpot chip obtained using a high speed camera. Note that the droplet is moving on a trajectory precisely perpendicular to the bottom surface of the chip and that no satellite droplets are formed. (b) Dispensing of nanolitre-droplets by a TopSpot dispenser having selectively coated outer surface. The coating prevents intermixing of solutions from different outlets and ensures long-term stable and well-defined dispensing properties of the device.

As an example, figure 10(a) shows a typical image sequence of the droplet formation indicating the formation of a single droplet. The selective hydrophobic coating effectively prevents formation of satellite droplets and leakage of fluid towards the outer surface of the print-head.

The image sequence displayed in figure 10(b) shows parallel operation of 24 nozzles (4 rows of 6 nozzles, only front row visible) and demonstrates homogeneity of droplet formation from a coated print-head. The distance between adjacent nozzles is  $500\ \mu\text{m}$ , droplet volume is about 1.2 nl.

Particularly with DNA-containing aqueous solutions, multiple printing operations may be performed without deterioration of spotting performance.

In contrast, proteins exhibit quite diverse properties and composition of printing solutions has to vary accordingly. Especially additives such as glycerol and amphiphiles which in some cases are required to stabilize proteins in solution render control of wettability and printing performance difficult. In these applications, purely hydrophobic coatings are insufficient to provide long-term control of wettability, since proteins tend to adsorb onto hydrophobic surfaces. Even though this process cannot be fully prevented from proceeding, the time scale on which print-head performance deteriorates may be extended by advanced coatings employing 3D micro- and nano-structures in combination with hydrophobic and protein-repellent coatings. Studies in this direction are currently under way in our laboratories.

#### 4. Summary and conclusions

Procedures for selective chemical surface modification applicable to a wide range of fluidic microsystems including micro-pipettes, nanotiter plates have been devised and coatings formed thereby have been characterized. Mixed layers from backfilling and especially from co-deposition of silane derivatives have shown enhanced stability with respect to acidic and particularly also basic solutions.

Selective chemical surface modification was shown to greatly enhance liquid handling performance of complex fluidic microsystems. Particularly, droplet dispensing from selectively modified micro-nozzles is reliable and long-term stable. Coated TopSpot systems have been cleaned and reused up to 60-fold.

Mostly due to cost considerations there is a trend towards the use of polymeric materials for the fabrication of micro-fluidic systems. However, many polymers exhibit hydrophobic surfaces which results in the task to devise procedures to render fluid channels wettable.

With the move from DNA-microarray technology to the fabrication of protein micro-arrays in addition to controlling the wettability of fluidic microsystems the issue of protein adsorption gains increasing importance. While DNA may be deposited from simple aqueous solutions, proteins exhibit a wide range of properties requiring equally diverse composition of printing solutions. Particularly amphiphilic compounds and glycerol as well as the tendency of proteins to adsorb on hydrophobic surfaces pose a considerable challenge to arrayer technology. To this end, ultra-hydrophobic surfaces and coatings with protein repelling properties are currently under development.

#### Acknowledgments

Funding for this study was in part obtained from the Government of Baden-Württemberg through grant no 720.430-21/15.

#### References

- [1] Gutmann O *et al* 2003 Droplet release in a highly parallel pressure driven nanoliter dispenser *IEEE Transducers (Boston, MA 2003)*

- [2] Becker H, Lowack L and Manz A 1998 Planar quartz chips with submicron channels for two-dimensional capillary electrophoresis applications *J. Micromech. Microeng.* **8** 24–8
- [3] Raymond D E, Manz A and Widmer H M 1996 Continuous separation of high molecular weight compounds using a microliter volume free-flow electrophoresis microstructure *Anal. Chem.* **68** 2515–22
- [4] Raymond D E, Manz A and Widmer H M 1994 Continuous sample pretreatment using a free-flow electrophoresis device integrated onto a silicon chip *Anal. Chem.* **66** 2858–65
- [5] Effenhauser C S, Manz A and Widmer H M 1993 Glass chips for high-speed capillary electrophoresis separations with submicrometer plate heights *Anal. Chem.* **65** 2637–42
- [6] Ramsey J M, Jacobson S C and Foote R S 1997 Applying the microelectronics paradigm to chemistry: the lab.-on-a-chip. *ISA Tech/Expo Technol. Update* (Research Triangle Park, NC: Instrument Society of America)
- [7] McKnight T E *et al* 2001 Electroosmotically induced hydraulic pumping with integrated electrodes on microfluidic devices *Anal. Chem.* **73** 4045–9
- [8] Griffiths S K and Nilson R H 2002 Design and analysis of folded channels for chip-based separations *Anal. Chem.* **74** 2960–7
- [9] Wang J *et al* 2003 Microchip capillary electrophoresis coupled with a boron-doped diamond electrode-based electrochemical detector *Anal. Chem.* **75** 935–9
- [10] Sakai-Kato K, Kato M and Toyooka T 2002 On-line trypsin-encapsulated enzyme reactor by the sol-gel method integrated into capillary electrophoresis *Anal. Chem.* **74** 2943–9
- [11] Sander L C, Callis J B and Field L R 1983 Fourier transform infrared spectrometric determination of alkyl chain conformation on chemically bonded reversed-phase liquid chromatography packings *Anal. Chem.* **55** 1068–75
- [12] Masada Y *et al* 1979 A novel method of preparing of glass capillary columns: low-temperature plasma etching and polymerization *HRC CC, J. High Resolut. Chromatogr. Chromatogr. Commun.* **2** 400–4
- [13] Pesek J J and Matyska M T 1996 Electrochromatography in chemically modified etched fused-silica capillaries *J. Chromatogr. A* **736** 255–64
- [14] Wirth M J and Fatunmbi H O 1993 Horizontal polymerization of mixed trifunctional silanes on silica: 2. Application to chromatographic silica gel. *Anal. Chem.* **65** 822–6
- [15] Kato M *et al* 2002 A protein-encapsulation technique by the sol-gel method for the preparation of monolithic columns for capillary electrochromatography *Anal. Chem.* **74** 1915–21
- [16] Rogers Y-H *et al* 1999 Immobilization of oligonucleotides onto a glass support via disulfide bonds: a method for preparation of DNA microarrays *Anal. Biochem.* **266** 23–30
- [17] Lamture J B *et al* 1994 Direct detection of nucleic acid hybridization on the surface of a charge coupled device *Nucleic Acids Res.* **22** 2121–5
- [18] Maskos U and Southern E M 1992 Oligonucleotide hybridisations on glass supports: a novel linker for oligonucleotide synthesis and hybridisation properties of oligonucleotides in situ *Nucleic Acid Res.* **20** 1679–84
- [19] Dodge A *et al* 2001 Electrokinetically driven microfluidic chips with surface-modified chambers for heterogeneous immunoassays *Anal. Chem.* **73** 3400–9
- [20] Gobet J and Kovats E 1984 Preparation of hydrated silicon dioxide for reproducible chemisorption experiments *Adsorption Sci. Technol.* **1** 77–92
- [21] Culler S R, Ishida H and Koenig J L 1985 Structure of silane coupling agents adsorbed on silicon powder *J. Coll. Interf. Sci.* **106** 334–46
- [22] Tripp C P and Hair M L 1995 Direct observation of the surface bonds between self-assembled monolayers of octadecyltrichlorosilane and silica surfaces: a low frequency IR study at the solid/liquid interface *Langmuir* **11** 1215–9
- [23] Le Grange J D and Markham J L 1993 Effects of surface hydration on the deposition of silane monolayers on silica *Langmuir* **9** 1749–53
- [24] Tripp C P and Hair M L 1992 An infrared study of the reaction of octadecyltrichlorosilane with silica *Langmuir* **8** 1120–6
- [25] Zhuravlev L T 1987 Concentration of hydroxyl groups on the surface of amorphous silicas *Langmuir* **3** 316–8
- [26] Hoffmann P W, Stelzle M and Rabolt J F 1997 Vapor Phase Self-Assembly of Fluorinated Monolayers on Silicon and Germanium Oxide *Langmuir* **13** 1877–80
- [27] Wirth M J and Fatunmbi H O 1992 Horizontal polymerization of mixed trifunctional silanes on silica: a potential chromatographic stationary phase *Anal. Chem.* **64** 2783–6
- [28] Azzam R M A and Bashara N M 1987 *Ellipsometry and Polarised Light* (Amsterdam: Elsevier Science)
- [29] Harke M, Stelzle M and Motschmann H R 1996 Microscopic ellipsometry: imaging monolayer on arbitrary reflecting supports *Thin Solid Films* **284–285** 412–6
- [30] Adamson A W 1990 *Physical Chemistry of Surfaces* (New York: Wiley)
- [31] Oliver J F, Huh C and Mason S G 1980 An experimental study of some effects of solid surface roughness on wetting *Coll. Surf.* **1** 79–104
- [32] Yaminsky V V, Claesson P M and Eriksson J C 1993 Wetting hysteresis and instability of hydrophobized glass and mica surfaces *J. Coll. Surf. Sci.* **161** 91–100
- [33] Brzoska J B, Azouz I B and Rondelez F 1994 Silanization of solid substrates: a step toward reproducibility *Langmuir* **10** 4367–73
- [34] Foti G, Belvito M L and Kovats E 1988 Packing density of organyldimethylsiloxy-covered silica gel and hydrolytic stability of the coating *J. Chromatogr.* **440** 315–22